Journal of Engineering and Computer Sciences
Vol. 17, No. 1, pp.29-39 (Jan 2025)

Investigation of Grid Distortion Effects on Motor Drives with Various Filter Topologies

Abdulrahman Alduraibi*
Department of Electrical Engineering, College of Engineering, Qassim University, Buraydah 52571, Saudi Arabia
E: mab.alduraibi@qu.edu.sa

[Received: 24 September, Revised: 06 October 2025, Accepted: 30 November 2025, Published Jan 2026]

Abstract: Variable frequency drives employing a three-phase diode rectifier front-end are widely used across various industrial networks due to their reliability and cost efficiency. Different filter topologies are implemented in these rectifiers to reduce current harmonics. Typically, these filters are designed for normal grid conditions without distortions. However, in the presence of grid distortion, their behavior can change significantly. This article examines how grid distortion affects current harmonic emission in motor drives with various filter topologies. First, a mathematical model of the rectified voltage is developed considering the presence of PCC voltage harmonics. Subsequently, simulation results are presented to assess the effect of distorted grids on different filter configurations. The results indicate that some filters, such as the AC and DC chokes, show substantial variations in current harmonics under grid distortion, primarily influenced by the phase angle of voltage harmonics. In contrast, the Electronic Inductor consistently maintained a stable THDi across various distorted grid scenarios, demonstrating its potential as an effective solution for VFDs operating in environments with grid distortion.

Keywords*:* Distorted grid, distribution networks, energy efficiency, total harmonic distortion

1. INTRODUCTION

Power electronics devices are being used more frequently in distribution networks. Among these devices is the Variable Frequency Drive (VFD), which can modify motor speed by changing its frequency and voltage. With an increased focus on boosting the efficiency of electric motors, which have been witnessed as one of the main consumers of global electricity [1]. The VFD has become extensively utilized in both industrial and commercial networks [2]. Despite the VFD's capability to greatly enhance motor efficiency, it produces significant current harmonics. The presence of current harmonics leads to elevated operating temperatures in distribution transformers. This thermal stress degrades the insulation integrity and significantly reduces the transformer's service life [3].

Front-end based on three phase diode rectifier is commonly used in VFD due to its reliability and low cost [4]. As a result, various filter topologies are implemented in these rectifiers to reduce current harmonics emissions. Passive filters, which include a large DC-link capacitor and DC or AC chokes, are commonly employed in many VFDs because of their reliability and simplicity. However, during partial power, which is common for most VFDs, the current harmonics produced by a VFD equipped with a passive filter are notably high [5]. Furthermore, the substantial size and limited lifespan of the DC-link capacitor present a major challenge in the power converter industry [6, 7]. Notably, it has been observed that up to 30% of power converter failures are attributable to the DC-link capacitor [7]. Recently, a small DC-link capacitor (SDLC) has gained researcher interest as a replacement of passive filter due to its compact size and longer life time [8, 9]. Moreover, SDLCs generate fewer current harmonics compared to traditional passive filters (DC choke or AC choke) [10]. Beyond these filtering methods, Electronic Inductors (EI) have attracted researchers as an economical active filter option for motor drives [11-13]. The EI involves placing a DC/DC boost converter as an intermediate circuit, simulating an infinite inductor to replace bulky passive filters [14]. However, it should be highlighted that the interaction of current harmonics with grid impedance leads to voltage harmonics at the Point of Common Coupling (PCC).

Additionally, the increasing use of renewable energy sources in distribution networks is leading to a rise in voltage harmonics [15, 16]. In [15], a microgrid powered by a photovoltaic (PV) station, replacing some linear loads with nonlinear loads resulted in a rise in total voltage harmonic distortion (THD_v) to 8%. Moreover, the field measurements of residential networks studied in [16] showed that 45% of the feeders have a THD_v higher than 5%, with an average THD_v of 4.7%. Additionally, the increased charging demand from electric vehicles contributes to the deterioration of voltage stability at the point of common coupling (PCC) in distribution networks [17]. Consequently, when VFDs operate in such distorted grids, they may produce current harmonics that differ significantly from the designed limits. In fact, international standards such as IEC61000-12-3 [18] impose strict requirements on voltage harmonics during VFD testing. Thus, the current harmonics emission of VFD should comply with the IEC61000-12-3 standard, as presented in Table 4 in [18]. However, in typical distribution networks, the voltage harmonics could be much higher than the voltage harmonics under test conditions of VFD.

Different studies have examined how unbalanced grid voltages and voltage sags affect the operation of VFDs [19-22]. It has been observed that under conditions of high grid voltage unbalance, VFDs equipped with passive filters may operate in a single-phase mode, generating elevated levels of current harmonics [20]. Additionally, in [22], the authors have shown that unbalanced grid voltages can increase stress on rectifier diodes and the DC-link capacitor. However, none of the reviewed literature investigates the impact of voltage harmonics on the VFD. While existing literature and standards such as IEEE-519 [23] have primarily focused on the magnitude of voltage harmonics, the critical influence of their phase angle remains largely unquantified in practical assessments of power quality. This gap is particularly relevant for modern non-linear loads like VFDs, whose harmonic emission behavior is sensitive to the phase relationship of the supply voltage harmonics. Authors in [24] investigated how voltage harmonics influence the current harmonic emissions of VFDs with passive filters (DC chokes), revealing that even small voltage harmonic levels can significantly affect current harmonics. The extent of current harmonic distortion can either increase or decrease depending on the phase angle of the voltage harmonics. However, given that typical distribution networks often contain numerous VFDs with various filtering topologies, it is crucial to study how voltage harmonics affect the current harmonic emissions across different VFD configurations.

Therefore, this article investigates the effects of PCC voltage harmonics on the current harmonics emission of VFD with different filter topologies. The distinct value of this work lies in its novel comparative framework that explicitly incorporates these phase-angle effects. Unlike conventional analyses, this study provides a more granular understanding of how specific phase-angle variations at the PCC influence VFD current harmonic emissions depending on filter configuration. These insights offer practical guidance for developing mitigation strategies that go beyond mere harmonic magnitude compliance. Consequently, four of the common filter configurations are considered in this paper. Different voltage harmonics order, magnitude, and phase-angle are considered in the study to achieve a comprehensive analysis. The rest of this article is organized as follows: Section 2 presents the mathematical modeling of the rectified voltage in a distorted grid. Section 3 analyzes the current harmonics of VFD with various filter topologies in a distorted grid, considering different scenarios. Finally, a conclusion of the study is presented in Section 4.

2. MATHEMATICAL MODELING OF THE RECTIFIED VOLTAGE IN DISTORTED GRID

Since the rectified voltage of the three-phase diode rectifier could be highly impacted by the distorted grid, which will then affect the current harmonics emission, the mathematical modeling of the rectified voltage under the presence of grid voltage harmonics needs to be first investigated. Thus, this section presents the mathematical modeling of the rectified voltage in a distorted grid based on the configuration shown in Fig. 1. In this scenario, the input voltage (PCC voltage) is

a combination of the fundamental voltage (V_1) and some of the harmonics (V_h). Hence, phase *a* voltage can be presented based on a sin-wave reference, as presented in (1).

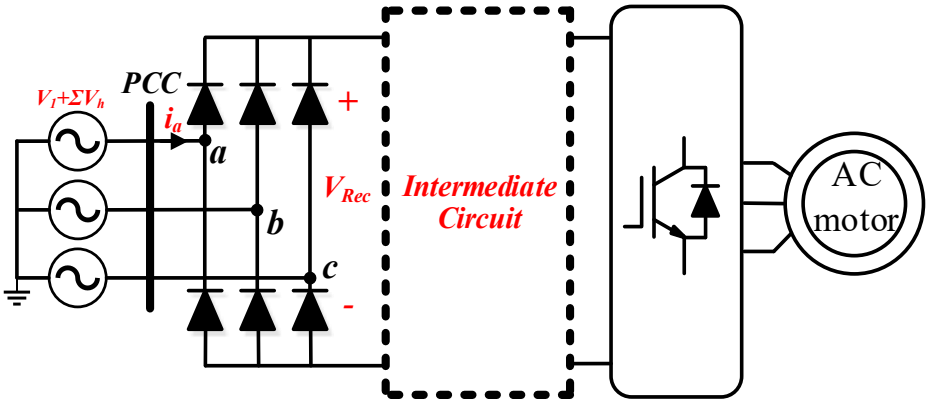

Fig. 1. VFD with three-phase diode rectifier front-end in distorted grid

$$v_{an} = V_m \sin(\omega t) + \sum_{h=2}^{\infty} V_h \sin(h\omega t + \theta_h) \tag{1}$$

Consequently, the rectified voltage (V_{Rec}) can be calculated based on Fourier series, considering the input voltage as presented in (1) and balanced voltage harmonics among all three phases, as giving in (2).

$$V_{Rec} = A_0 + \sum_{n=1}^{\infty} (A_n \cos(6n\omega t) + B_n \sin(6n\omega t)) \tag{2}$$

Where the A_o represents the DC component of the rectified voltage and can be calculated as in (3) and A_n and B_n represent the AC components of the rectified voltage and can be calculated as in (4) and (5) respectively. In equations (3), (4), and (5) there is a coefficient defined as δ which is the commutation delay caused by the phase-angle of the voltage harmonics as presented in Fig.2. This commutation delay shifts the conductivity of the three phases by δ (measured in radian) which could impact the displacement power factor. The commutation delay (δ) can be calculated based on (6) where ωt_o can be found by solving (7). Equation (7) is derived by setting the instantaneous voltages of phases *a* and *c* equal to each other.

$$A_0 = \frac{3\sqrt{3}V_m}{\pi} cos\,\delta + \sum_{h=2}^{\infty} \frac{12V_h}{\pi h} sin\left(\frac{2\pi}{3}h\right) sin\left(\frac{\pi}{6}h\right) cos(h\delta + \theta_h) \tag{3}$$

$$\begin{aligned} A_n = {} & \frac{3\sqrt{3}V_m\, cos(n\pi)}{\pi(36n^2-1)}[(6n-1)\,cos(6n\delta+\delta) - (6n+1)\,cos(6n\delta-\delta)] \\ & + \frac{12}{\pi}\sum_{h=2}^{\infty} V_h\, cos(n\pi)\, sin\left(\frac{2\pi}{3}h\right) sin\left(\frac{\pi}{6}h\right)\left[\frac{cos(6n\delta+h\delta+\theta_h)}{6n+h}\right. \\ & \left. - \frac{cos(6n\delta-h\delta-\theta_h)}{6n-h}\right] \end{aligned} \tag{4}$$

$$B_n = \frac{3\sqrt{3}V_m\, cos(n\pi)}{\pi(36n^2-1)}[(6n-1)\, sin(6n\delta+\delta) - (6n+1)\, sin(6n\delta-\delta)] + \frac{12}{\pi}\sum_{h=2}^{\infty} V_h\, cos(n\pi)\, sin\left(\frac{2\pi}{3}h\right) sin\left(\frac{\pi}{6}h\right)\left[\frac{sin(6n\delta+h\delta+\theta_h)}{6n+h} - \frac{sin(6n\delta-h\delta-\theta_h)}{6n-h}\right] \quad (5)$$

$$\delta = \omega t_0 - \pi/6 \quad (6)$$

$$\sqrt{3}\, V_m \cos\left(\omega t_0 + \frac{\pi}{3}\right) + \sum_{h=2}^{\infty}[2V_h \cos\left(h\omega t_0 + \theta_h + \frac{h\pi}{3}\right) \sin\left(\frac{h\pi}{3}\right)] = 0 \quad (7)$$

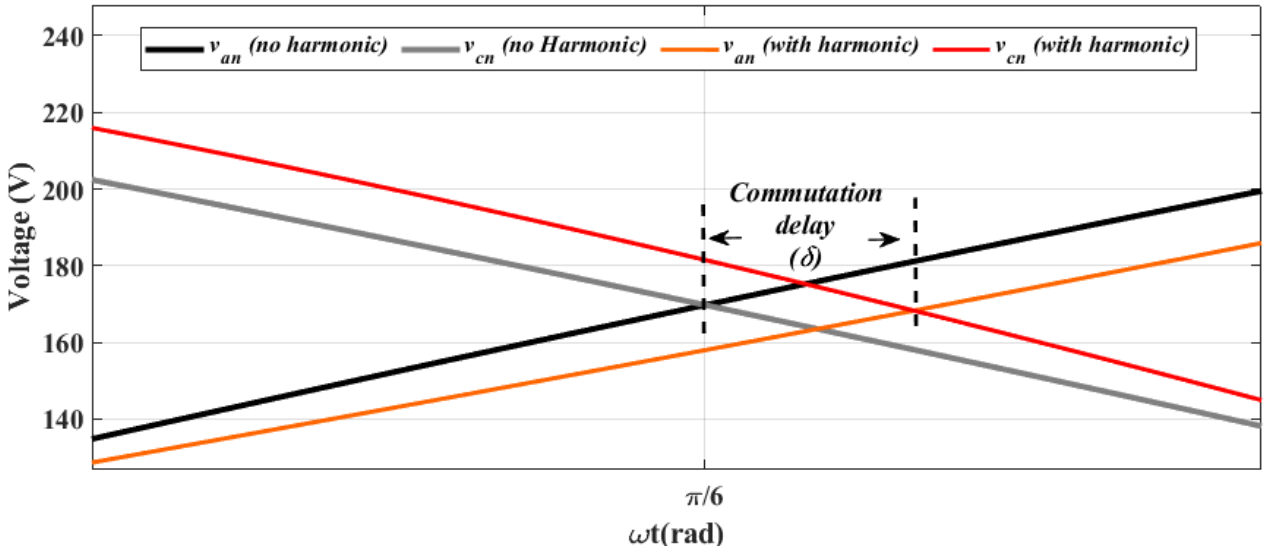

Fig. 2. The commutation delay (δ) caused by the voltage harmonics phase-angle

To illustrate the numerical solution for the commutation delay, for simplicity, only 5% of the 5th voltage harmonic with a 90˚ phase angle (θ_h) is considered when solving equation (7). As a result, solving equation (7) yields an ωt_o of 32.782˚. Consequently, the commutation delay can be determined by substituting this ωt_o value into equation (6), resulting in a commutation delay of 2.782˚. It is important to note that the commutation delay exists when the voltage harmonic's phase angle is any value other than 0˚ or 180˚. When the phase angle is 0˚ or 180˚, the commutation delay will be zero.

To validate the mathematical modeling of the rectified voltage (V_{Rec}) presented in equations (2) to (7), a time-domain waveform of the rectified voltage is presented in Fig. 3. In this figure, a comparison is made between the mathematical model of rectified voltage and simulation results using MATLAB Simulink. Two cases have been considered in this validation: Case 1, when the grid voltage is distorted by 5% of the 5th voltage harmonics with zero phase angle as shown in Fig.3 (a) and in Case 2, the grid voltage is distorted by 5% of the 5th voltage harmonics with 180˚ phase angle as shown in Fig.3 (b). As can be seen from the figure, the mathematical model is consistent with the simulation results, which validate the proposed mathematical model.

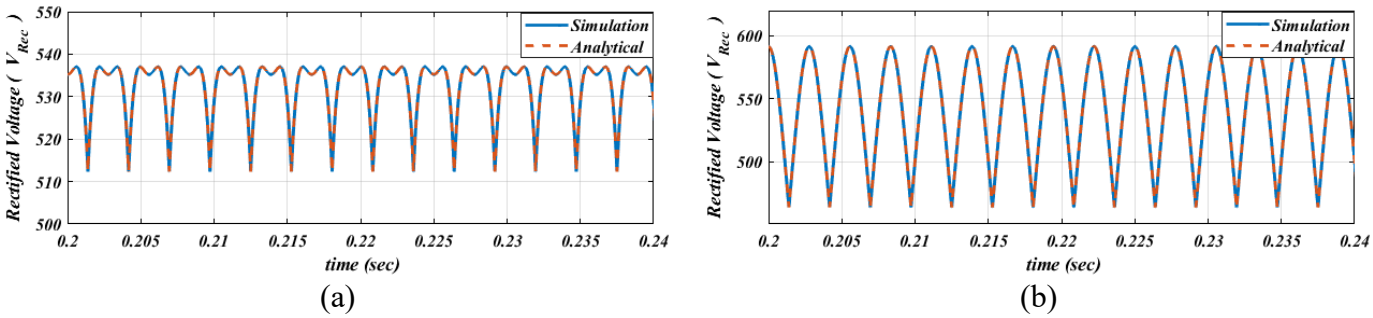

Fig. 3. Comparison between mathematical model and simulation of the rectified voltage in distorted grid; (a) 5% of 5th harmonic with 0˚ phase angle, (b) 5% of 5th harmonic with 180˚ phase angle

3. HARMONIC ANALYSIS OF VFD IN DISTORTED GRID

As noted in the introduction, VFD often use a three-phase diode rectifier as their front-end converter. To reduce current harmonics emission, various filter topologies are employed. Therefore, this section examines four common filters. Fig. 4 illustrates the filter topologies used in the analysis: a) AC choke, b) DC choke, c) Small DC-link capacitor, and d) Electronic Inductor (EI). The filters are designed based on the allowable harmonics emission standards, with the AC choke tailored to 3% of the base impedance at rated power and the DC choke designed at 5%. The Small DC-link capacitor is typically less than 100µF. The EI functions as an active filter using a boost converter designed with a dual-loop controller, featuring a PI controller for output voltage regulation in the outer loop and a hysteresis controller for inductor current control in the inner loop. The parameters for the VFD units depicted in Fig.4 are listed in Table 1. All units maintain consistency by being equipped with a 10 kW motor drive system.

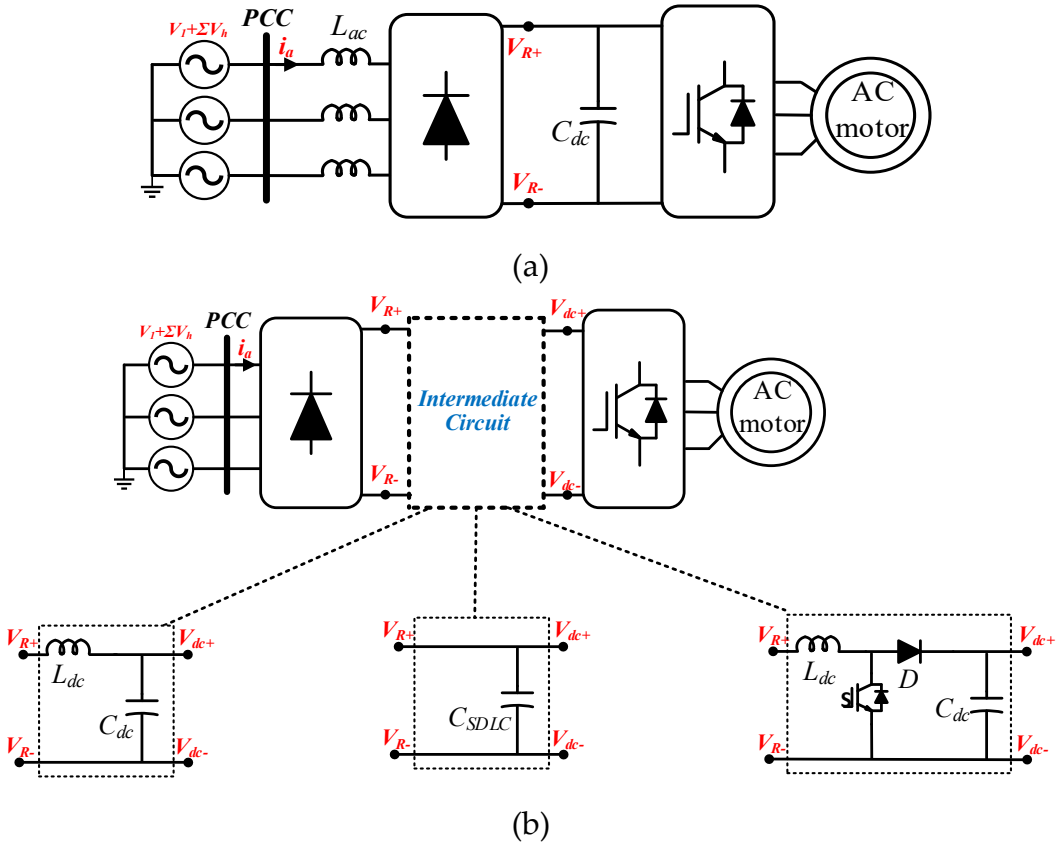

Fig. 4. VFD with different filter topologies; (a) AC choke, (b) DC choke, (c) SDLC, (d) EI

Table 1. Parameters of VFD units, which are presented in Fig. 4

Symbol	Parameter	Value
	Grid Parameters:	
v_{abc}	Phase voltage	230 V_{rms}
f_g	frequency	60 Hz
Z_g	Grid impedance	0.01Ω,128 μH
	AC choke:	
L_{ac}	AC inductor	1.2 mH
C_{dc}	DC-link Capacitor	360 μF
	DC choke:	
L_{dc}	DC-link inductor	1.8 mH
C_{dc}	DC-link Capacitor	470 μF
	SDLC:	
C_{SDLC}	Small DC-link Capacitor	25 μF
	EI:	
L_{dc}	DC-link inductor	2 mH
C_{dc}	DC-link Capacitor	560 μF
V_{dc}	Output voltage	700 V_{dc}
K_p, k_i	PI parameters	5, 0.08

To examine how a distorted grid affects the current harmonics emission of VFD with various filter topologies, this analysis considers five scenarios featuring different grid distortions, as outlined in Table 2. These scenarios incorporate common voltage harmonics found in industrial grids (5th and 7th harmonic orders). Although the phase angle of these voltage harmonics can be unpredictable due to factors such as the type of nonlinear loads and grid impedance, this study uses phase angles of 0˚ and 180˚ to assess their impact on current harmonics emission. Case 1 serves as the baseline with no distortion for comparison. Table 2 shows that the phase angle significantly affects rectified voltage ripple. In cases 2 and 3, there is an approximate 65% increase in ripple compared to Case 1, when no voltage harmonics exist at the PCC. Consequently, some filter topologies may experience worsened current harmonics. Conversely, in cases 4 and 5, the ripple decreases by about 40% to 60% relative to Case 1, potentially leading to improved current harmonics emission.

Table 2. Investigated cases' details

Case	PCC voltage harmonics (%)	V_{Rec} ripple (V)
1	No voltage harmonics	66
2	V_{h5}=5∠0˚	25.6
3	V_{h5}=5∠180˚	110
4	V_{h7}=5∠0˚	109
5	V_{h7}=5∠180˚	39

Table 3 details the current harmonic emission of the four common filter topologies under varying grid voltage distortions. The data indicate that passive filters with AC and DC chokes exhibit high sensitivity to these distortions. This sensitivity applies not only to the magnitude of the distortion but also to the phase angle of the voltage harmonics. For instance, in Case 2, where the 5th harmonic phase angle is 0˚, the THDi for the AC and DC choke filters is lower than in the baseline scenario with no voltage harmonics (Case 1). Conversely, in Case 3, when the 5th harmonic phase angle shifts to 180˚, the THDi increases significantly compared to the baseline. The SDLC filter demonstrates a similar trend, though with a much smaller variation in THDi. In contrast, the THDi of the EI filter remains stable across all tested grid distortion conditions.

Table 3. Current harmonic emission under different grid voltage distortions at rated power

Case	*PCC voltage distortion (%)*	*Units' THDi (%)*			
		AC Choke	*DC choke*	*SDLC*	*EI*
1	**No voltage harmonics**	**44.8**	**46.5**	**33.6**	**29.4**
2	V_{h5}=5∠0˚	32	30	31	29.1
3	V_{h5}=5∠180˚	59.6	69.2	37.1	29.6
4	V_{h7}=5∠0˚	60.4	74	37	29
5	V_{h7}=5∠180˚	32.9	30.5	35.6	29.6

The grid current waveforms for phase "a" are illustrated for the first three cases in Figures 5, 6, 7, and 8, corresponding to four different filter topologies: AC choke, DC choke, SDLC, and EI, respectively. Fig. 5 shows that the AC choke experiences significant current ripple variation when the voltage harmonic phase angle changes. In Case 2, when Vh5=5%∠0° is introduced to the PCC voltage, the current ripple reduces with 32% THDi. Conversely, when Vh5=5%∠180° is applied, the current ripple increases, raising the THDi to 59.6%. A similar trend is seen with the DC choke, which exhibits slightly more variation, as Fig. 6 demonstrates. In Case 2, the THDi is reduced to 30%, while in Case 3, the THDi rises sharply to 69.2%. The SDLC maintains minimal current ripple variation with only slight changes in THDi across the three cases, as shown in Fig. 7. Finally, the EI topology displays stable current ripple throughout all three cases, maintaining a constant THDi of 29%, as shown in Fig.8.

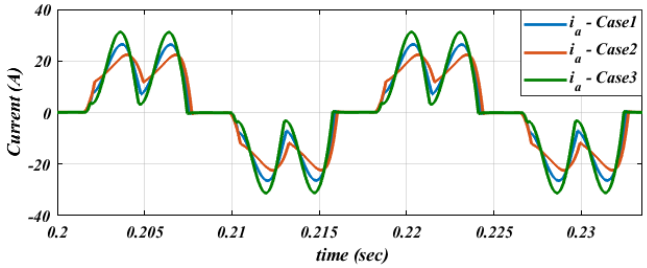

Fig. 5. AC-choke filter grid current waveforms at rated power for the first three cases

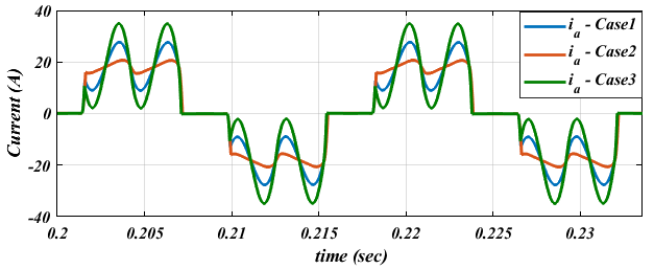

Fig. 6. DC-choke filter grid current waveforms at rated power for the first three cases

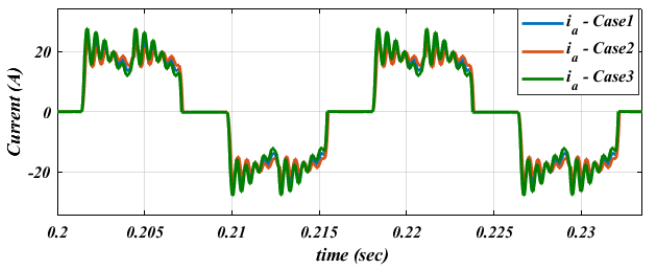

Fig. 7. SDLC filter grid current waveforms at rated power for the first three cases

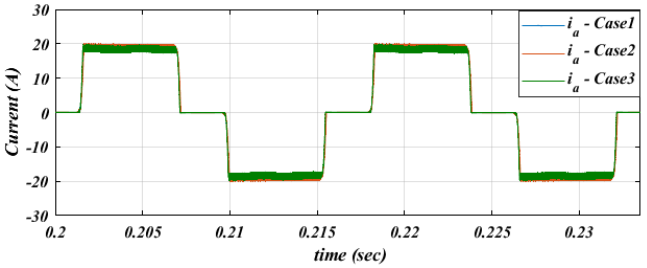

Fig. 8. EI filter grid current waveforms at rated power for the first three cases

Finally, considering that motor drives typically function at partial power much of the time, it is important to explore how a distorted grid affects VFD current harmonic emission under partial power conditions. Therefore, the scenarios outlined in Table 2 are used to investigate filter performance when the motor operates at 50% of its rated power. Fig. 9 and Table 4 display the THDi percentages for the four types of filters across the five cases. The results indicate that the filters exhibit trends similar to those at rated power; however, the variation in THDi levels for the AC and DC chokes has increased. For instance, with the DC choke, THDi in Case 2 drops significantly to 34% compared to 76% in Case 1 (no distortion),

while in Case 3, it rises to 90.7%. The SDLC shows a slightly greater variation in THDi at partial power than at full power. It is notable that the AC choke, DC choke, and SDLC have higher THDi levels at partial power than at full power across the five cases. Conversely, the EI maintains a steady THDi level of around 30% in both partial and rated power conditions for all the cases examined.

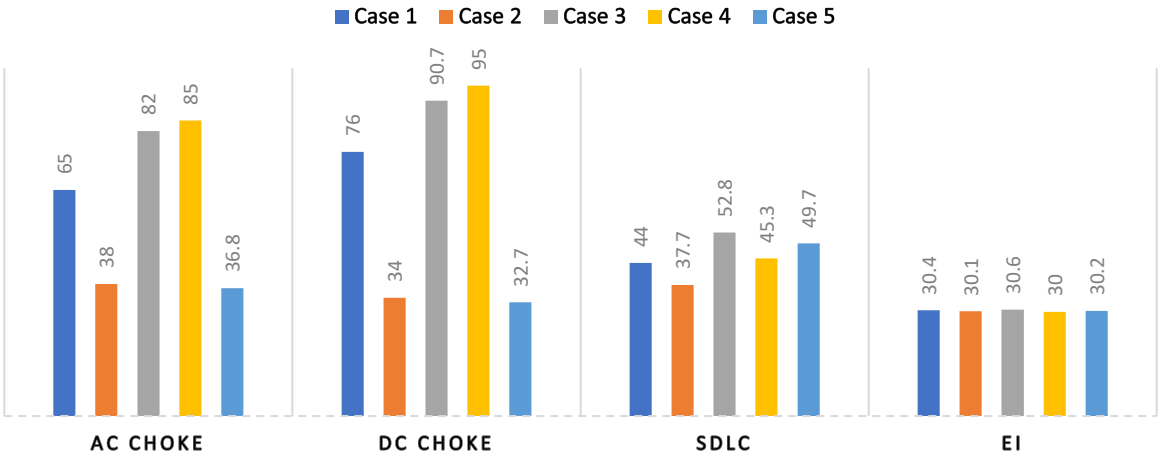

Fig. 9. THDi values of grid current of all filter topologies for all 5 cases under 50% of the rated power

Table 4. Current harmonic emission under different grid voltage distortions at 50% of rated power

Case	*PCC voltage distortion (%)*	*Units' THDi (%)*			
		AC Choke	*DC choke*	*SDLC*	*EI*
1	**No voltage harmonics**	**65**	**76**	**44**	**30.4**
2	V_{h5}=5∠0°	38	34	37.7	30.1
3	V_{h5}=5∠180°	82	90.7	52.8	30.6
4	V_{h7}=5∠0°	85	95	45.3	30
5	V_{h7}=5∠180°	36.8	32.7	49.7	30.2

Figures 10-13 show phase-a grid current waveforms for the first three cases under partial power (50%), each corresponding to a different filter: AC choke, DC choke, SDLC, and EI. The figures show the filters follow similar trends observed at rated power. Fig. 10 indicates the AC choke's current ripple is highly sensitive to the voltage harmonic phase angle: adding V_{h5} = *5%∠0°* at the PCC (Case 2) reduces THDi to 38%, while V_{h5} = *5%∠180°* increases THDi to 82% and the current operates at Discontinuous Conduction Mode (DCM). The DC choke, presented in Fig. 11, follows a similar but slightly larger variation; the THDi falls to 34% in Case 2 and jumps to 90.7% in Case 3 with DCM current. The SDLC, presented in Fig. 12, shows minor ripple changes, with THDi varying slightly across cases. The EI topology remains the most stable, keeping current ripple and THDi constant at 30% in all three cases, as shown in Fig. 13.

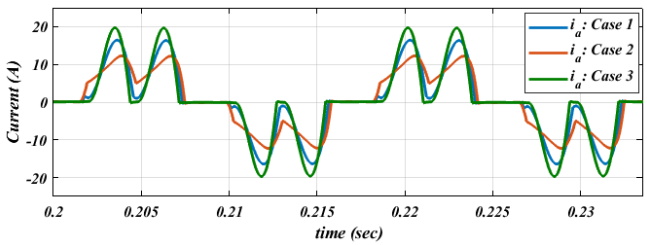

Fig. 10. AC-choke filter grid current waveforms at partial power for the first three cases

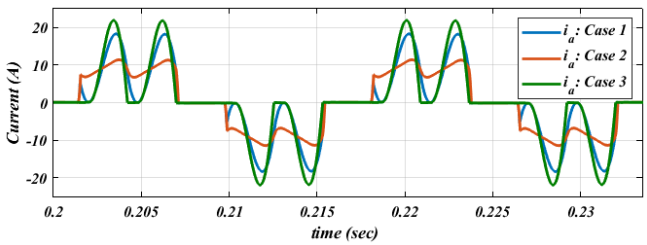

Fig. 11. DC-choke filter grid current waveforms at partial power for the first three cases

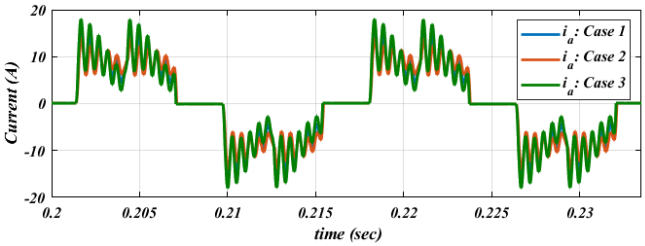

Fig. 12. SDLC filter grid current waveforms at partial power for the first three cases

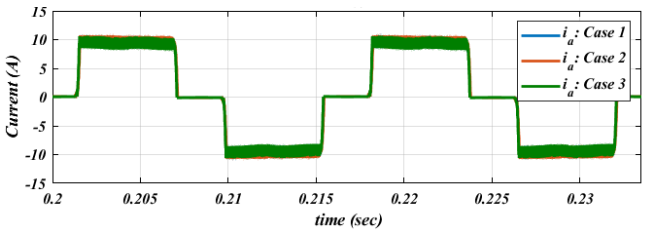

Fig. 13. EI filter grid current waveforms at partial power for the first three cases

To sum up, the filter topologies used in VFDs exhibit varying responses to grid distortion. Passive filters like the AC and DC chokes are significantly influenced by the grid distortion, with their effects dependent on the phase angle of voltage harmonics. The phase angle can either greatly enhance or worsen the emission of current harmonics. The Small DC-Link Capacitor (SDLC) demonstrates relatively better performance under distorted grid conditions, with only slight variations in current harmonic emission. Conversely, the Electronic Inductor (EI) maintains a consistent THDi across different grid distortion scenarios, indicating its potential as a promising solution for VFD applications in distorted grids. Furthermore, international standards such as IEC 61000-3-12 [18] and IEEE 519 [23] specify the allowable levels of voltage harmonics at the PCC of distribution networks without considering the phase angle's influence. As evidenced by the cases studied herein, the phase angle of the voltage harmonics at the PCC has a significant impact on the current harmonic emission of VFDs.

4. CONCLUSION

This study investigated the impact of grid voltage distortion on variable frequency drives equipped with four common filter topologies. A mathematical model of the rectified voltage was developed to account for PCC voltage harmonics, and various grid distortion scenarios were simulated to evaluate each filter's performance. The key finding for practical application is that filter selection is critical and depends heavily on the expected grid conditions. The results demonstrate that passive filters, such as AC and DC chokes, exhibit significant sensitivity to both the magnitude and, more importantly, the phase angle of voltage harmonics. This sensitivity can lead to unpredictable and elevated THDi, making them a higher-risk choice for installations in highly distorted or unstable grids. Conversely, the Electronic Inductor filter maintained a stable and low THDi across all tested distortion scenarios. This reliability makes it a robust and recommended solution for engineers designing VFD systems for industrial environments where grid power quality is poor or uncertain. Therefore, for practitioners prioritizing performance stability and compliance with harmonic standards in real-world conditions, the EI filter presents a superior and more dependable option than traditional passive chokes. The results, obtained using MATLAB Simulink to emulate various types of grid distortion, provide a strong foundational analysis. To enhance the practical applicability of these findings, future work should include validation through industrial measurements. Furthermore, while this study focused on harmonic emissions at the unit level, system-level interactions could alter harmonic behavior. Therefore, investigating current harmonic emission in a distorted grid at the system level represents a valuable direction for future research.

REFERENCES

[1] P. Waide and C. U. Brunner, "Energy-efficiency policy opportunities for electric motor-driven systems," 2011.
[2] B. K. Bose, "Power electronics and motor drives recent progress and perspective," *IEEE Transactions on Industrial Electronics,* vol. 56, pp. 581-588, 2009.
[3] M. S. Seddik, M. B. Eteiba, and J. Shazly, "Evaluating the harmonic effects on the thermal performance of a power transformer," *Energies,* vol. 17, p. 4871, 2024.

[4] T. Friedli, M. Hartmann, and J. W. Kolar, "The essence of three-phase PFC rectifier systems—Part II," *IEEE Transactions on Power Electronics,* vol. 29, pp. 543-560, 2014.
[5] D. Kumar and F. Zare, "Harmonic analysis of grid connected power electronic systems in low voltage distribution networks," *IEEE Journal of Emerging and Selected Topics in Power Electronics,* vol. 4, pp. 70-79, 2016.
[6] K. Kuang, X. Guo, C. Li, X. Li, X. Xi, and H. Fang, "A novel multiscale perspective based hotspot temperature assessment method for film capacitor in DC-link applications," *IEEE Transactions on Industry Applications,* vol. 60, pp. 9111-9122, 2024.
[7] M. M. Ramees and M. W. Ahmad, "Advances in capacitor health monitoring techniques for power converters: A review," *IEEE Access,* vol. 11, pp. 133540-133576, 2023.
[8] M. Hinkkanen and J. Luomi, "Induction motor drives equipped with diode rectifier and small DC-link capacitance," *IEEE Transactions on Industrial Electronics,* vol. 55, pp. 312-320, 2008.
[9] W.-J. Lee and S.-K. Sul, "DC-link voltage stabilization for reduced DC-link capacitor inverter," *IEEE Transactions on industry applications,* vol. 50, pp. 404-414, 2013.
[10] F. Zare, H. Soltani, D. Kumar, P. Davari, H. A. M. Delpino, and F. Blaabjerg, "Harmonic emissions of three-phase diode rectifiers in distribution networks," *Ieee Access,* vol. 5, pp. 2819-2833, 2017.
[11] Y. Yang, P. Davari, F. Blaabjerg, and F. Zare, "Load-independent harmonic mitigation in SCR-fed three-phase multiple adjustable speed drive systems with deliberately dispatched firing angles," *IET Power Electronics,* vol. 11, pp. 727-734, 2018.
[12] A. Sunbul, F. Zare, R. Sharma, and A. Ghosh, "A comprehensive steady-state analysis for modular multi-parallel rectifiers (MMR) with shared DC-link," *IEEE Transactions on Industry Applications,* vol. 59, pp. 1969-1981, 2022.
[13] A. Alduraibi, J. Yaghoobi, D. Solatialkaran, and F. Zare, "A Modular Power Converter with Active Front End System to Mitigate Harmonics in Distribution Networks," *IEEE Journal of Emerging and Selected Topics in Power Electronics,* 2020.
[14] P. Davari, Y. Yang, F. Zare, and F. Blaabjerg, "A review of electronic inductor technique for power factor correction in three-phase adjustable speed drives," in *2016 IEEE Energy Conversion Congress and Exposition (ECCE)*, 2016, pp. 1-8.
[15] P. N. Korovesis, G. A. Vokas, I. F. Gonos, and F. V. Topalis, "Influence of large-scale installation of energy saving lamps on the line voltage distortion of a weak network supplied by photovoltaic station," *IEEE transactions on power delivery,* vol. 19, pp. 1787-1793, 2004.
[16] K. D. McBee and M. G. Simoes, "Evaluating the long-term impact of a continuously increasing harmonic demand on feeder-level voltage distortion," *IEEE Transactions on Industry Applications,* vol. 50, pp. 2142-2149, 2013.
[17] M. N. Iqbal, L. Kütt, K. Daniel, B. Asad, and P. Shams Ghahfarokhi, "Estimation of harmonic emission of electric vehicles and their impact on low voltage residential network," *Sustainability,* vol. 13, p. 8551, 2021.
[18] IEC, "IEC 61000-3-12, Electromagnetic compatibility (EMC) – Part 3-12: Limits – Limits for harmonic currents produced by equipment connected to public low-voltage systems with input current >16 A and ⩽75 A per phase," ed: IEC, 2011.
[19] K. Lee, G. Venkataramanan, and T. M. Jahns, "Source current harmonic analysis of adjustable speed drives under input voltage unbalance and sag conditions," *IEEE transactions on power delivery,* vol. 21, pp. 567-576, 2006.
[20] D. Kumar, P. Davari, F. Zare, and F. Blaabjerg, "Analysis of three-phase rectifier systems with controlled DC-link current under unbalanced grids," in *Applied Power Electronics Conference and Exposition (APEC), 2017 IEEE*, 2017, pp. 2179-2186.
[21] H. Wang, P. Davari, D. Kumar, F. Zare, and F. Blaabjerg, "The impact of grid unbalances on the reliability of DC-link capacitors in a motor drive," in *2017 IEEE Energy Conversion Congress and Exposition (ECCE)*, 2017, pp. 4345-4350.
[22] L. B. Fisch, O. H. Gonçalves, F. Trentini, C. A. Hummelgen, and A. J. Rossa, "Impact analysis on variable-speed drives under unbalanced grid conditions," in *2023 IEEE 8th Southern Power Electronics Conference and 17th Brazilian Power Electronics Conference (SPEC/COBEP)*, 2023, pp. 1-8.
[23] "IEEE Standard for Harmonic Control in Electric Power Systems," *IEEE Std 519-2022 (Revision of IEEE Std 519-2014),* pp. 1-31, 2022.
[24] A. Alduraibi, J. Yaghoobi, and F. Zare, "Impacts of Grid Voltage Harmonics Amplitude and Phase Angle Values on Power Converters in Distribution Networks," *IEEE Access,* vol. 9, pp. 92017-92029, 2021.

دراسة آثار تشوه الشبكة على المحركات بأنواع مرشحات مختلفة

تُستخدم محركات التردد المتغير المزودة بمقوّم ثلاثي الطور أمامي بالديود على نطاق واسع في الشبكات الصناعية المختلفة لما تتمتع به من موثوقية وكفاءة في التكلفة. تُطبق انواع مرشحات مختلفة في هذه المقومات لتقليل التوافقيات في التيار. عادةً ما تُصمَّم هذه المرشحات لظروف شبكة طبيعية خالية من التشوهات. ومع ذلك، في حالة وجود تشوه بالشبكة، يمكن أن يتغير سلوكها بشكل كبير. تفحص هذه المقالة كيفية تأثير تشوهات الشبكة على انبعاث التوافقيات في التيار في محركات القيادة ذات انواع مرشحات مختلفة. أولاً، يتم تطوير نموذج رياضي للجهد المقرّب مع الأخذ في الاعتبار وجود توافقيات جهد عند نقطة الاتصال المشترك. بعد ذلك، تُعرض نتائج المحاكاة لتقييم تأثير الشبكات المشوّهة على تكوينات المرشحات المختلفة. تشير النتائج إلى أن بعض المرشحات، مثل ملفات الحث على التيار المتردد وملفات الحث على التيار المستمر، تظهر تغيّرات كبيرة في توافقيات التيار تحت تشوّه الشبكة، ويتأثر ذلك بشكل أساسي بزوايا طور توافقيات الجهد. في المقابل، حافظ الملف الإلكتروني الحثّي باستمرار على إجمالي توافقيات التيار مستقراً عبر سيناريوهات شبكية مشوّهة متنوعة، مما يُبرز إمكاناته كحلّ فعّال لمحركات التردد المتغير العاملة في بيئات تعاني من تشوه الشبكة.